

Time-dependent behaviours of railway prestressed concrete sleepers in a track system

Li, Dan; Kaewunruen, Sakdirat; You, Ruilin

DOI:

[10.1016/j.engfailanal.2021.105500](https://doi.org/10.1016/j.engfailanal.2021.105500)

License:

Creative Commons: Attribution-NonCommercial-NoDerivs (CC BY-NC-ND)

Document Version

Peer reviewed version

Citation for published version (Harvard):

Li, D, Kaewunruen, S & You, R 2021, 'Time-dependent behaviours of railway prestressed concrete sleepers in a track system', *Engineering Failure Analysis*, vol. 127, 105500. <https://doi.org/10.1016/j.engfailanal.2021.105500>

[Link to publication on Research at Birmingham portal](#)

General rights

Unless a licence is specified above, all rights (including copyright and moral rights) in this document are retained by the authors and/or the copyright holders. The express permission of the copyright holder must be obtained for any use of this material other than for purposes permitted by law.

- Users may freely distribute the URL that is used to identify this publication.
- Users may download and/or print one copy of the publication from the University of Birmingham research portal for the purpose of private study or non-commercial research.
- User may use extracts from the document in line with the concept of 'fair dealing' under the Copyright, Designs and Patents Act 1988 (?)
- Users may not further distribute the material nor use it for the purposes of commercial gain.

Where a licence is displayed above, please note the terms and conditions of the licence govern your use of this document.

When citing, please reference the published version.

Take down policy

While the University of Birmingham exercises care and attention in making items available there are rare occasions when an item has been uploaded in error or has been deemed to be commercially or otherwise sensitive.

If you believe that this is the case for this document, please contact UBIRA@lists.bham.ac.uk providing details and we will remove access to the work immediately and investigate.

Time-dependent behaviours of railway prestressed concrete sleepers in a track system

1 **Dan Li^{1,2}, Sakdirat Kaewunruen^{1,2*}, Ruilin You³**

2 ¹ Department of Civil Engineering, School of Engineering, University of Birmingham, Birmingham
3 B15 2TT, United Kingdom

4 ² TOFU Lab (Track engineering and Operations for Future Uncertainties), School of Engineering,
5 University of Birmingham, Birmingham B15 2TT, United Kingdom

6 ³ Railway Engineering Institute, China Academy of Railway Sciences, Beijing 100081, China

7 *** Correspondence:**

8 Sakdirat Kaewunruen

9 S.Kaewunruen@bham.ac.uk

10 **Abstract**

11 The main functions of railway sleepers are: (i) to safely transfer loads from wheel axles to foundation;
12 (ii) to secure both rails ensuring correct track gauge at all time; and, (iii) to restrain movements of rails
13 to control longitudinal creeps. In reality, railway industry can experience costly problems of railseat
14 twists and tight gauges, for instance, due to time-dependent actions and poor workmanship. These
15 problems prevent trains to navigate over tracks safely, effectively and quietly. They require additional,
16 expensive maintenance activities much more frequently over time such as rail renewal, rail
17 reprofiling/grinding, rail pad replacement, curve lubrication adjustment, etc. On this ground, it is very
18 important to maintain the geometry and topological/dimensional stability of railway sleepers. The long-
19 term geometric performance of sleepers can be significantly influenced by time-dependent actions and
20 behaviours. The creep and shrinkage in prestressed concrete sleepers result in internal actions that is
21 led to geometric deformation, which change the rail gauge and influence the safety and reliability of
22 track components. Time-dependent behaviours also lead to increased complex internal stresses, which
23 can cause cracking on prestressed concrete railway sleepers. The cracks stemming from creep and
24 shrinkage can be observed in real life, at a certain time after construction, along the sleepers and near
25 the fasteners such as anchorage, bolt holes, and web openings. In this study, unprecedented
26 experimental and numerical investigations are conducted to evaluate time-dependent behaviours of
27 full-scale prestressed concrete sleepers. An empirical calculation method is also introduced and the
28 empirical results are compared with both experimental and numerical results. Insights into creep and
29 shrinkage effects are highlighted in order to essentially aid predictive and preventative track
30 maintenance, supporting the effective and efficient decision making of both (i) engineers and
31 manufacturers and (ii) infrastructure managers and owners.

32 **Keywords:** prestressed concrete sleeper, creep, shrinkage, time-dependent behaviour, finite element
33 method (FEM), numerical analysis, experiment, Eurocode

34

35

36 **1 Introduction**

37 Railway transportation is believed to be the safest transportation system for both passengers and goods
38 and provides a safe, economical, and comfortable ride. Ballast railway track is the most common
39 railway track structure used around the world. Typical ballasted railway track can be categorized into
40 superstructure and substructure, as shown in **Figure 1**. The superstructure consists of rails, rail pads,
41 prestressed concrete sleepers, and fastening systems. The substructure includes ballast, sub-ballast, and
42 formation. It is important for both the superstructure and sub-structure to ensure the safety and comfort
43 of the ride. The structural element that distributes vertical loads from rails to the substructure is the
44 sleeper. Traditional railway sleepers can be manufactured from timber, concrete, steel, and any other
45 engineered materials. Prestressed concrete sleepers are the most popular type in railway track around
46 world because of its structural performance [1-20]. The main functions of sleepers are: to maintain rail
47 gauge; to transfer and distribute vertical loads from rails to the underlying ballast bed; to restrain
48 longitudinal, lateral, or vertical movement; and to hold and support rails [21].

49 Long-term performance of prestressed concrete sleepers can be influenced by many factors, such as
50 deterioration, cracking from dynamic loads, fatigue, and environmental or chemical degradation [22,
51 23]. Sadeghi, J evaluated railway sleepers for its sufficient strength to sustain the environmental and
52 traffic loads. Improvements by the incorporation of long-term effect were suggested in railway sleeper
53 design [24]. Time-dependent behaviour can also significantly influence long-term performance of
54 prestressed concrete. Creep and shrinkage can cause cracking of railway sleepers due to loss of
55 prestress, deterioration, and increasement of internal pressure, which reduces the service life.

56 Creep and shrinkage of concrete were discovered in the early 20th century and have many very complex
57 influential factors. Creep is the increasement of strain over time when the concrete structure is loaded.
58 Shrinkage is the volume of concrete structure being reduced due to loss of water [25]. In recent decades,
59 many researchers have tried to investigate mechanisms of creep and shrinkage, but they still cannot be
60 fully understood.

61 The most important aspects to investigate when it comes to creep and shrinkage are material and
62 structural analysis. In terms of material, researchers are trying to find more accurate predict model. In
63 structural terms, the effect of creep and shrinkage will be studied. A number of experiments has been
64 conducted to study creep and shrinkage in recent decades. There has been an improvement in the
65 theoretical prediction and the analysis of the effects of creep and shrinkage. Presently, various design
66 codes are predicting time-dependent behaviour such as Eurocode 2, ACI, and the Australian Standard.
67 However, each code considering different parameters focuses on regional situation.

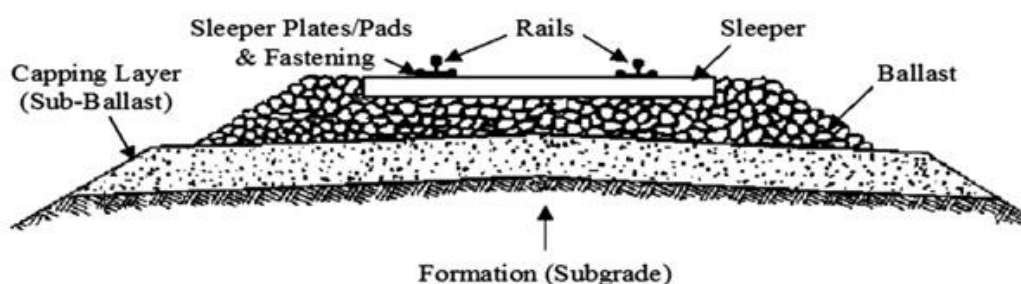
68 Investigators usually believe that creep and shrinkage have significant effects on long-span concrete
69 structures. Most research on creep and shrinkage has focused on prestressed concrete bridge girders.
70 W. He [26] stated creep and shrinkage affect camber development in prestressed bridge girders. Byle
71 et al [27] monitored the long-term deformation of pretensioned high performance concrete bridge
72 girders. Beam cambers and deflections, concrete strains, and concrete temperatures were monitored on
73 girders in the bridge to estimate long-term behaviour. The analytical time-step method was used to
74 predict time-dependent behaviour. A multi-scale method was utilized by Lopez [28] to investigate
75 time-dependent deformation of prestressed concrete girders.

76 However, few researchers investigate time-dependent behaviour of prestressed concrete railway
77 sleepers. The design process and effect factors are considered very different from prestressed concrete
78 girders. Therefore, time-dependent behaviour of railway sleeper cannot be analysed like bridge girders.

79 Prestressed concrete sleeper is a very important component of railway track systems. As a prestressed
 80 concrete structure, the performance can be influenced by time-dependent behaviour. In the long-term,
 81 the deformation due to time-dependent behaviour can induce rail change. This deformation also leads
 82 to loss of prestress and reduces the capacity of concrete. Structural damages occur, such as cracks,
 83 which are the warning signs of structural failure.

84 This study focuses on deformation due to time-dependent behaviour because the critical dimension of
 85 railway sleepers can be significantly affected by creep and shrinkage. In this paper, a numerical study
 86 is rigorously executed to comprehensively evaluate time-dependent deformation on prestressed
 87 concrete sleepers. Experimental studies of reliability concepts for the time-dependent deformation are
 88 presented. The prediction concept based on Eurocode 2 is introduced as a method of theoretical analysis.
 89 The research also carries out statistical and probabilistic studies to investigate time-dependent
 90 behaviour.

91



92

93 **Figure 1.** Ballasted railway track structure

94 **2 Theoretical time-dependent behaviour prediction method**

95 Eurocode 2 [29] describes prediction methods of creep and shrinkage, which are utilised to calculate
 96 the theoretical results of creep and shrinkage.

97 **2.1 Creep**

98 The total creep strain $\varepsilon_{cc}(t, t_0)$ of concrete due to the constant compressive stress of σ_c applied at the
 99 concrete age of t_0 is given by:

$$100 \quad \varepsilon_{cc}(t, t_0) = \varphi(t, t_0) \times \frac{\sigma_c}{E_c} \quad (1)$$

101 where:

102 $\varphi(t, t_0)$ is the final creep coefficient;

103 σ_c is the compressive stress.

104 E_c is the tangent modulus.

$$105 \quad \varphi(t, t_0) = \varphi_{RH} \times \frac{16.8}{\sqrt{f_{cm}}} \times \frac{1}{(0.1 + t_0^{0.20})} \quad (2)$$

$$106 \quad \varphi_{RH} = 1 + \frac{1-0.01 \times RH}{0.1+h_0^{0.333}}, f_{cm} \leq 35MPa \quad (3)$$

$$107 \quad \varphi_{RH} = \left(1 + \frac{1-0.01 \times RH}{0.1+h_0^{0.333}} \alpha_1\right) \alpha_2, f_{cm} > 35MPa \quad (4)$$

$$108 \quad \alpha_1 = \left(\frac{35}{f_{cm}}\right)^{0.7}, \alpha_2 = \left(\frac{35}{f_{cm}}\right)^{0.2} f_{cm} = f_{ck} + 8MPa \quad (5)$$

$$109 \quad t_0 = t_{0,T} \left(\frac{9}{2+t_{0,T}^{1.2}}\right)^\alpha \geq 0.5, \alpha = \{-1(S), 0(N), 1(R)\} \quad (6)$$

110 where:

111 φ_{RH} is the relative humidity coefficient.

112 RH is relative humidity in percentage;

113 h_0 is the ratio of cross-sectional area and perimeter of the member in contact with the atmosphere,
114 $h_0 = 2A_c/u$;

115 S, R and N refer to different classes of cement.

116 2.2 Shrinkage

117 The total shrinkage strain ε_{cs} can be given by:

$$118 \quad \varepsilon_{cs} = \varepsilon_{ds} + \varepsilon_{as} \quad (7)$$

119 where:

120 ε_{ds} is drying shrinkage strain; ε_{as} is autogenous shrinkage strain.

121 The drying shrinkage strain ε_{ds} can be estimated by:

$$122 \quad \varepsilon_{ds} = \beta_{ds}(t, t_0) \times \varepsilon_{cd0} \times k_h \quad (8)$$

$$123 \quad \varepsilon_{cd0} = 0.85[(220 + 110\alpha_{ds1}) \times \exp(-\alpha_{sd2} \times 0.1f_{cm})] \times 1.55[1 - (0.01RH)^3]10^6 \quad (9)$$

$$124 \quad \beta_{ds}(t, t_0) = \frac{(t-t_s)}{(t-t_s)+0.04\sqrt{h_0^3}} \quad (10)$$

125 where:

126 k_h is coefficient which depends on the national size h_0 ;

127 RH is relative humidity in percentage;

128 $h_0 = 2A_c/u$ in mm, A_c is cross sectional area, u is the perimeter of the member in contact with the
129 atmosphere;

130 The values of parameter α_{ds1} and α_{ds2} as a function of the type of cement are shown as **Table 2**.

Cement type	α_{ds1}	α_{ds2}
S	3	0.13
N	4	0.12
R	6	0.11

131 **Table 2.** Cement type and coefficient

132 The autogenous shrinkage strain ε_{as} can be calculated from:

133
$$\varepsilon_{as} = \beta_{as}(t) \times \varepsilon_{ca}(\infty) \quad (11)$$

134
$$\varepsilon_{ca}(\infty) = 2.5 \times (f_{ck} - 10) \times 10^{-6} \quad (12)$$

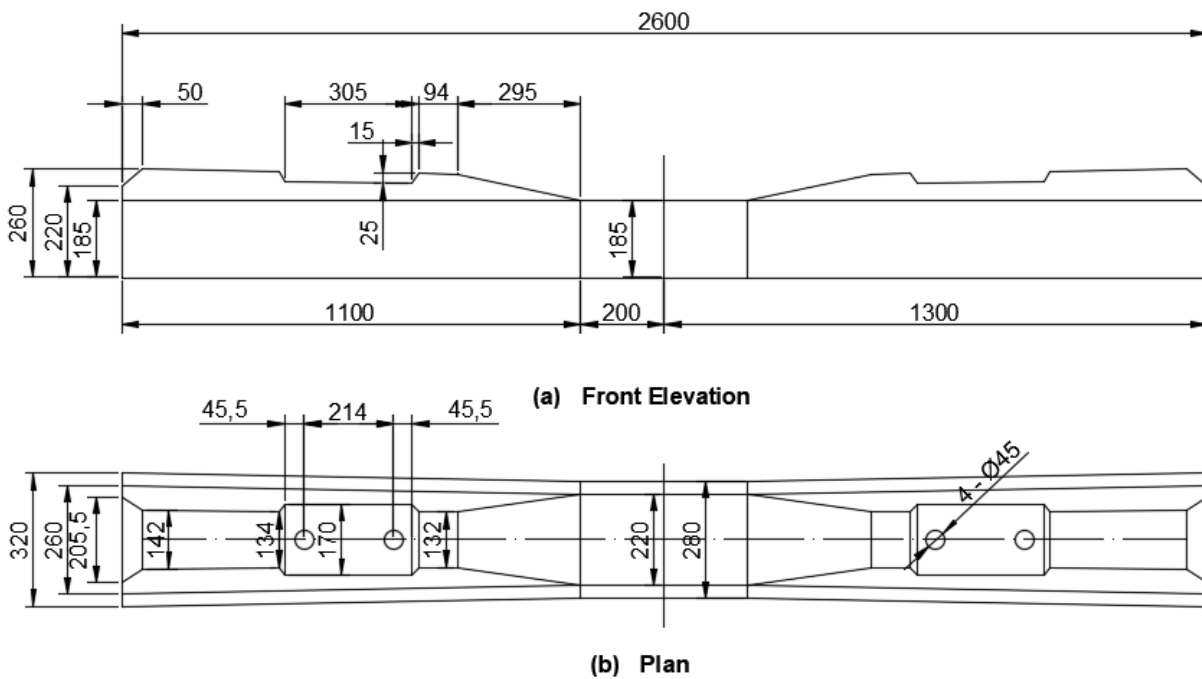
135
$$\beta_{as}(t) = 1 - \exp(-0.2t^{0.5}) \quad (13)$$

136

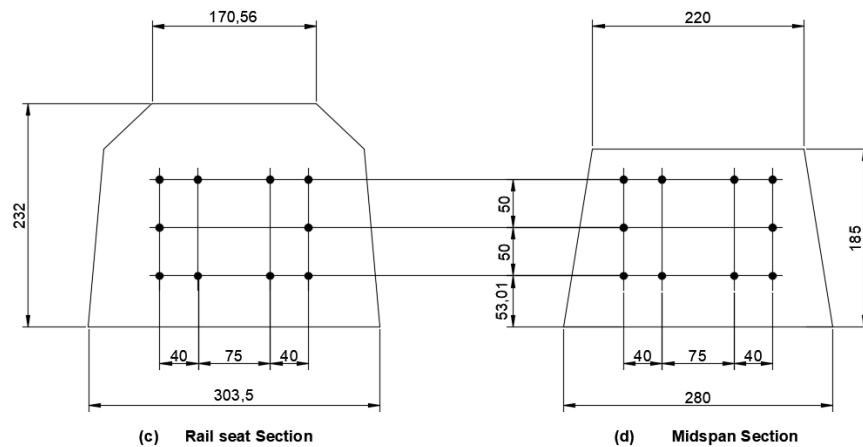
137 3 Type III prestressed concrete sleeper details

138 In this study, the 2600 mm long Chinese Type III prestressed concrete sleeper are analysed. The
 139 geometric details of the sleeper are shown in **Figure 2**. Dimension information for the selected
 140 prestressed concrete sleeper is shown below:

- 141 (a) Track gauge: 1435 mm;
 142 (b) Concrete strength class: 42.5
 143 (c) Distance between rail seats: 1818 mm



144



145

146

Figure 2. Chinese Type III prestressed concrete sleeper geometric details

147

Cement type	Basic variables	Value
Concrete properties	Mean compressive strength	65Mpa
	Modulus of elasticity	33Gpa
	Yield strength	1570Mpa
	Modulus of elasticity	200Gpa

148

Table 3. Material properties

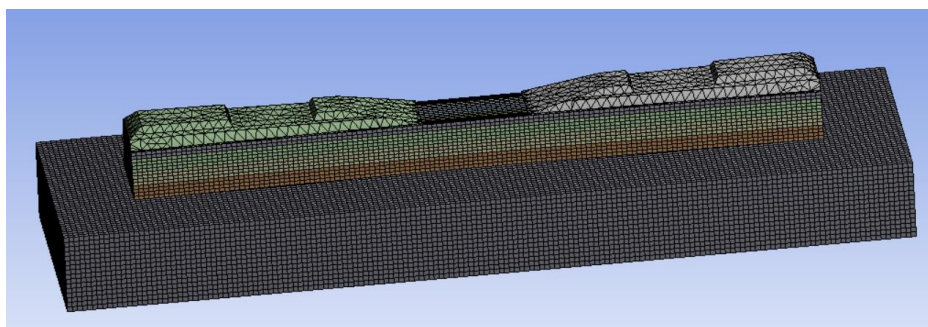
149

150

151 4 Finite element modelling

152 4.1 Finite element model details

153 The finite element models in this paper are developed by Ansys Workbench. The model consists of
 154 three parts: sleeper, ballast, and tendons. The finite element model is shown in **Figure 3**. In this research,
 155 concrete and ballast (block) are modelled as solid elements. Prestressed tendons are modelled as beam
 156 elements. In this FE model, concrete, prestressed tendons, and ballast are assumed to have perfect
 157 contact. The material parameters of FEM are shown in **Table 4**.



158

159

Figure 3. Finite element model of Chinese Type III prestressed concrete sleeper

160

Parts	Modulus of elasticity (Mpa)	Density (kg/m ³)	Poisson's ratio
Sleeper	33000	2400	0.23
Ballast	33000	2400	0.30
Tentons	200000	9800	0.30

161

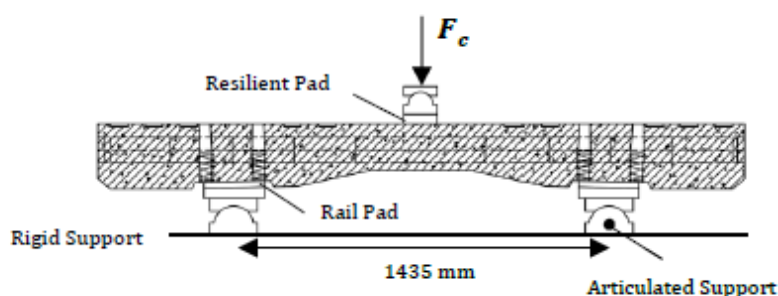
Table 4. Material parameters of FEM

162 4.2 Element types, boundary conditions and loading

163 In total, the model consists of 33921 nodes and 12246 elements, with most of these elements being 10-
 164 node tetrahedron elements. In the model, the boundary conditions are No Separation, where the
 165 concrete, prestressing tendons, and ballast are assumed to be well adhered. The bottom interface of
 166 ballast is set as fixed support. In this study, the external loads are not considered for time-dependent
 167 behaviour. Therefore, the Standard Earth Gravity is applied at the FEM. The Thermal Condition is
 168 used to simulate prestressing force transfer.

169 4.3 Finite element sleeper model validation

170 In this step, the static capacity test of sleeper [30] is used to validate the material and structural
 171 properties of FE sleeper model. The simulation of time-dependent behaviour will be conducted when
 172 FE sleeper model has been validated. An experimental programme was conducted at Beijing Jiaotong
 173 University by Professor Jing's group. **Figure 4** shows the apparatus for this centre negative moment
 174 test of sleeper. The results of load-deflection responses for the prestressed concrete sleeper at centre,
 175 obtained from this experiment using digital image correlation (DIC), are utilised to evaluate the mesh
 176 sensitivity of FE model. The fracture results are used to validate the failure mode of the FE sleeper
 177 model.



178

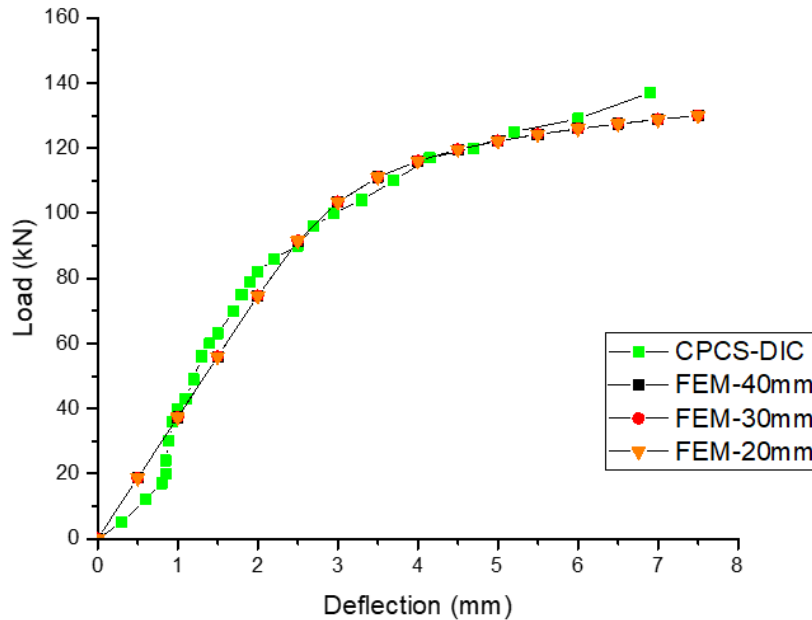
Figure 4. Apparatus of centre negative moment test of sleeper

180

181 4.3.1 Mesh size validation

182 In order to validate the FE prestressed concrete sleeper model, mesh sizes of 20mm, 30mm, and 40mm
 183 are attempted to use in sleeper model to analyse the mesh sensitivity. The results of load-deflection

184 responses (including experimental data and FEM) at the centre of prestressed concrete sleeper are
 185 plotted in **Figure 5**.



186

187 **Figure 5.** Load-deflection responses of prestressed concrete sleeper at rail centre section

188 **Figure 5** shows the load-deflection responses between FEM 20mm, 30mm, and 40mm are slightly
 189 different. The 30mm mesh size is selected, in comparison with the DIC (experimental) results, this
 190 mesh size similar and close (with 5.99% max error). It can be seen that FE results accurately meets
 191 experimental data.

192 4.3.2 Failure mode validation

193 To complete the validation process, failure mode validation needs to be conducted. As we know,
 194 concrete starts cracking when the load exceeds maximum tensile strength. **Figure 6** shows *Normal*
 195 *Stress* distribution on the X axis of the FE model. In **Figure 6** the red area represents tensile zoom and
 196 the blue area is compressive zoom. With displacement increasing, the stresses also become larger.
 197 Once the X axis stress in tensile zoom reaches the tensile strength of the sleeper, it can be assumed to
 198 be cracking (failure). In this step, the tensile strength is calculated by the theoretical design standard
 199 (Eurocode 2) [28]. The tensile strength will be used for determining cracking load and deflection in
 200 FEM results in order to compare this with experimental cracking load/deflection. The mean value
 201 tensile strength of concrete f_{ctm} is given by:

$$202 \quad f_{ctm} = 2.12 \ln(1.8 + 0.1 \times f_{ck}) \quad (14)$$

203 where f_{ck} is compressive strength of concrete.

204 The tensile strength is calculated as equal to 4.49 MPa, and the sleeper is assumed to start cracking
 205 after this point. The stress/load-deflection responses of mesh size 30mm FE model are illustrated in
 206 **Figure 7** in order to obtain cracking load. From **Figure 7**, the cracking deflection is 1.09mm when the
 207 X axis stress meets 4.49MPa. Therefore, the cracking load is 42.16kN. In the centre negative moment

208 test of the sleeper, the first cracking was observed at 45kN and from **Figure 5** (CPCS-DIC) the cracking
 209 deflection was at 1.13mm. The comparison between experimental and FE results is shown in **Table 5**.

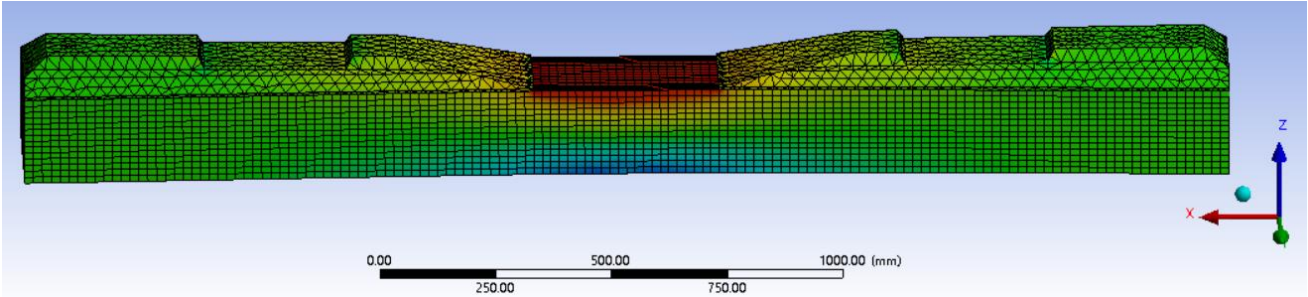
210

Cracking load	Experiment	FE					
	45kN	Size 20mm		Size 30mm		Size 40mm	
		kN	Deviation	kN	Deviation	kN	Deviation
		42.12	6.39%	42.16	6.30%	42.03	6.61%

211

Table 5. Comparison cracking loads between experiment and FE

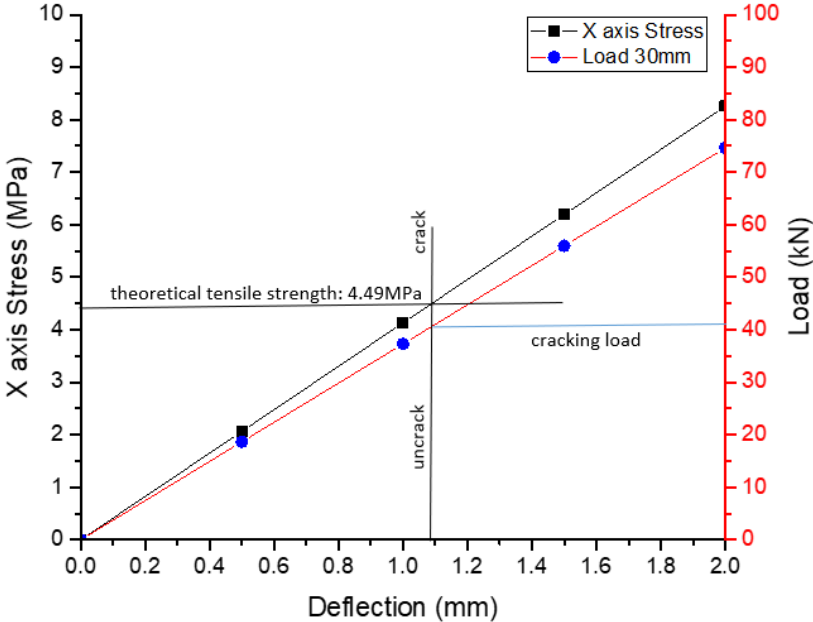
212



213

214

Figure 6. Normal stress distribution through X axis



215

216

Figure 7. The stress/load-deflection responses of mesh size 30mm FE model

217

218 4.4 Analysis settings

219 4.4.1 Creep numerical model

220 In this study, the Creep Rate Equation is chosen to simulate the effect of creep. The equations consider
 221 the creep strain rate, which can be a function of stress, strain, temperature, and neutron flux level. The
 222 Time-hardening of *Creep Strain Rate Model* adopts the following functions:

$$223 \dot{\varepsilon}_{cr} = C_1 \sigma^{C_2} \varepsilon_{cr}^{C_3} e^{-C_4/T} \quad (15)$$

224 where:

225 $\dot{\varepsilon}_{cr}$ is change in equivalent creep strain with respect to time;

226 ε_{cr} is equivalent creep strain;

227 σ is equivalent stress;

228 T is temperature (absolute);

229 C_1, C_2, C_3, C_4 are constants.

230 The implicit method is used to analyse creep, which is robust, fast, accurate, and recommended for
 231 general use. The implicit method can model pure creep, creep with isotropic hardening plasticity, and
 232 creep with kinematic hardening plasticity, using both von Mises and Hill potentials. Where the material
 233 model combination with creep is supported, any of the implicit creep models can be used.

234 4.4.2 Shrinkage numerical model

235 Shrinkage consists of plastic shrinkage and drying shrinkage. Plastic shrinkage happens in the first few
 236 hours after placing concrete. Drying shrinkage is mainly due to loss of water by evaporation and this
 237 lasts perhaps for years after the prestressed concrete sleeper is put in service. Therefore, the shrinkage
 238 numerical model focuses on drying shrinkage simulation. The *Thermal Condition* are used in the
 239 shrinkage simulation. In this method, thermal deformation is used to predict time-dependent shrinkage
 240 shortening by changing temperature. The shrinkage shortening at specific time (in days) is converted
 241 to temperature. The prediction equation is shown below:

$$242 T = -250 + a * \exp(b * t) \quad (16)$$

243 where T is temperature that converts time-dependent shrinkage to thermal shortening;

244 t is time which unit in days;

245 a, b are constants.

246 5 Experiment

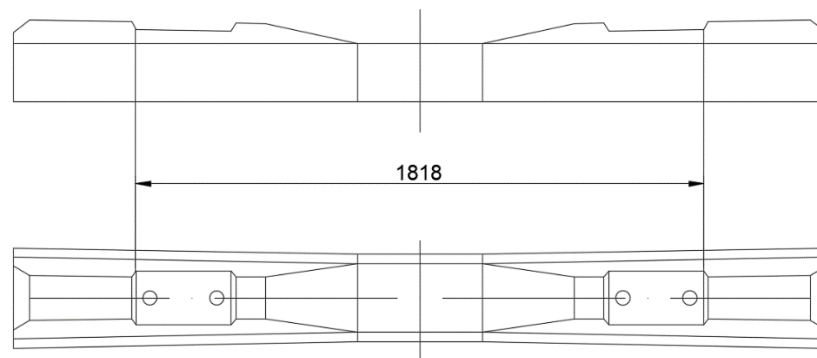
247 To evaluate the performance of prestressed concrete sleepers on time-dependent behaviour, an
 248 experiment was conducted at a concrete sleeper factory in Hebei province, China. Five Chinese Type
 249 III prestressed concrete sleepers were randomly selected since demoulding in sleeper factory. The
 250 sleepers were standard gauge which commonly used in ballasted railway in China. A series of static
 251 tests on the prestressed sleepers were performed in accordance with Eurocode 2. The average

252 compressive strength of demoulding concrete was 62MPa and the elastic modulus was 36500MPa.
253 Each prestressing tendon with 7mm in diameter has a specified minimum proof force of 420kN.

254 To research deformation on prestressed concrete sleeper due to time-dependent behaviour, the critical
255 dimension is measured so as to observe the change with time. This experiment lasted for 180 days. The
256 setup for testing is illustrated in **Figure 8**. The distance between edge of rail seats is regarded as critical
257 dimension which is 1818mm shown in **Figure 8**. In this investigation, the critical dimension
258 measurement was arranged at 0, 7, 28, 35, 42, 49, 56, 60, 90, 180 days. The vernier calliper was utilised
259 to conduct measurement. **Figure 9** shows critical dimension measurement of specimens conducted in
260 sleeper factory. It should be noted that the measuring position for each specimen need to be marked in
261 first measurement. This step guarantees the following testing would be carried out at same position to
262 avoid human errors.

263 It should also be noted that the discreteness during the testing. Many influential factors could lead to
264 the experimental results various. For example, in practice, the compressive strength and elastic
265 modulus of concrete are varying with time. Even in same curing conditions, the material properties
266 could be different. The theoretical methods consider several main parameters and the value is constant.
267 Environmental factor is the most difficult to control. The relative humidity measurement was also
268 carried out which average value is approximate 70%. In fact, relative humidity could change every
269 hour and it can also be affected by seasonal variation. Therefore, more than three specimens are
270 suggested to test for average results.

271



272

273

Figure 8. setup for time-dependent behaviour testing

274



Figure 9. Sleeper critical dimension measurement

275

276

277

278 6 Results and discussion

279 6.1 Theoretical results

280 The theoretical results were calculated for 40 years according to Eurocode 2 (the equation shown in
 281 Part 2). The information of material properties and sleeper structure were following Chinese Type III
 282 prestressed concrete sleeper details (shown in Part 3). The calculation of sleeper deformation was
 283 divided into two parts: centre and side. The length of centre sleeper is 400mm and both sides length is
 284 709mm utilised to calculate the deformation. The width is determined by the cross-section of the
 285 sleeper. 75% relative humidity was applied in the theoretical calculation. The theoretical results of
 286 time-dependent behaviour are shown in **Table 6**.

Time (days)	Creep (mm)	Shrinkage (mm)	Total shortening (mm)
1	0.114	0.043	0.16
3	0.184	0.082	0.27
7	0.245	0.136	0.38
28	0.371	0.289	0.66
60	0.458	0.398	0.86
90	0.507	0.454	0.96
180	0.594	0.534	1.13
365	0.675	0.587	1.26
1095	0.766	0.626	1.39
1825	0.791	0.634	1.43
3650	0.814	0.640	1.45
7300	0.826	0.643	1.47
14600	0.832	0.644	1.48

287 **Table 6.** Theoretical results of time-dependent behaviour

288 6.2 Experimental results

289 The deformation between edges of rail seats were recorded for 180 days (shown in **Table 7**). The
290 average deformation was also calculated in order to compare the theoretical and numerical results.

Time	X-1	X-2	X-3	X-4	X-5	Average
<i>(days)</i>	<i>(mm)</i>	<i>(mm)</i>	<i>(mm)</i>	<i>(mm)</i>	<i>(mm)</i>	<i>(mm)</i>
0	0	0	0	0	0	0
7	0.4	0.6	0.4	0.6	0.3	0.46
28	0.6	0.9	0.5	0.7	0.6	0.66
35	0.6	0.9	0.6	0.8	0.6	0.7
42	0.6	1	0.6	0.8	0.6	0.72
49	0.6	1.1	0.6	1	0.8	0.82
56	0.65	1.1	0.7	0.95	0.8	0.84
60	0.7	1.1	0.8	0.9	0.8	0.86
90	0.9	1	0.8	1.1	0.9	0.94
180	1.1	0.9	1	1.2	0.95	1.03

291 **Table 7.** Experimental results of time-dependent behaviour

292

293 6.3 Numerical results

294 The numerical models for time-dependent behaviour simulation were introduced in Part 4.4. The
295 computation was carried out in Ansys Workbench. The time-dependent deformation, including creep
296 and shrinkage, was respectively calculated for 10 years (3650 days) shown in **Table 8**.

Time	Creep	Shrinkage	Total shortening
<i>(days)</i>	<i>(mm)</i>	<i>(mm)</i>	<i>(mm)</i>
1	0.11439	0.01049	0.12488
3	0.18807	0.08915	0.27722
7	0.26182	0.12631	0.38813
28	0.3817	0.30038	0.68208
90	0.47508	0.42187	0.89695
180	0.53366	0.5257	1.05936
365	0.58838	0.54688	1.13526
1095	0.66287	0.58199	1.24486
3650	0.73918	0.61668	1.35586

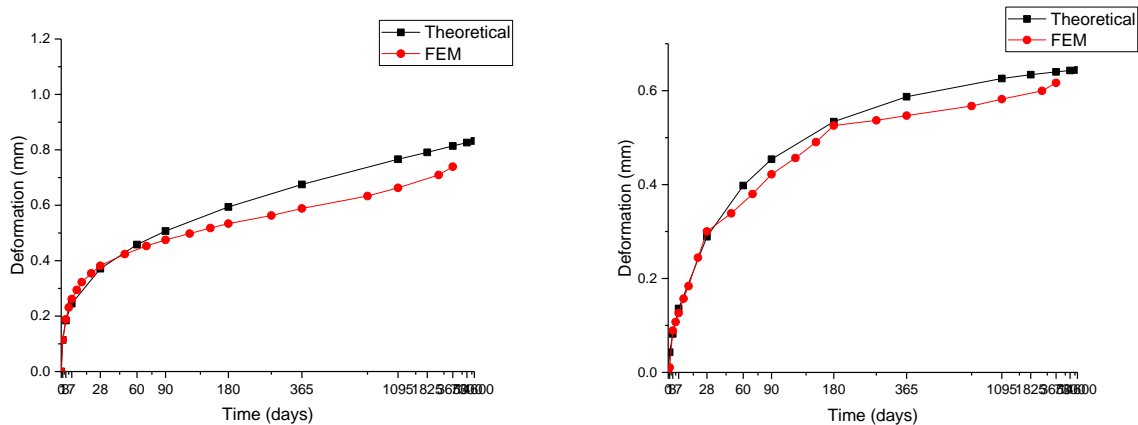
297 **Table 8.** Numerical results of time-dependent behaviour

298 6.4 Discussion

299 **Figure 10** shows a comparison between time-dependent deformation results of theoretical time-
300 dependent behaviour prediction method and the numerical model for 10 years (3650 days). It is clear
301 seen that both of creep and shrinkage increase with time. In early age, deformation increases sharply
302 and after 3 years (1095 days) increasement of deformation becomes very slow. From **Figure 10**, the

303 deformation due to creep is higher than shrinkage, which creep has more effect on sleeper dimension
 304 than shrinkage. The results of the numerical models for both of creep and shrinkage can be compared
 305 against theoretical results on which the model is calibrated. The numerical models should at least be
 306 able to estimate time-dependent behaviour well. The maximum errors between theoretical and
 307 numerical results for creep and shrinkage deformation prediction are 13.46% and 7.03% respectively.

308 The 180-day experimental results are illustrated in **Figure 11** in order to validate FEM model and
 309 theoretical method. Experimental results present time-dependent deformation including creep and
 310 shrinkage. Therefore, theoretical and numerical results need to combine creep and shrinkage results in
 311 order to compare with experimental data. In **Figure 11**, both theoretical and numerical predictions are
 312 quite close to the experimental results while maximum errors for theoretical and numerical results in
 313 comparison with experimental data are 8.85% and 4.58% respectively. The comparison between the
 314 experimental and numerically obtained time-dependent deformation curves indicates that the
 315 numerical model is able to predict the development of time-dependent behaviour.



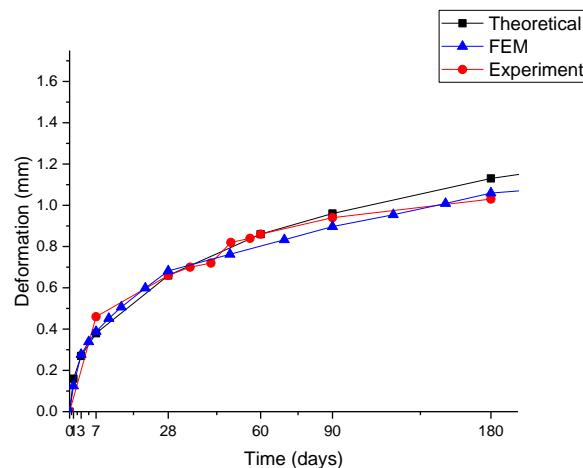
316

(a) creep deformation

(b) shrinkage deformation

317

318 **Figure 10.** Comparison between theoretical and numerical results of creep and shrinkage for 10 years



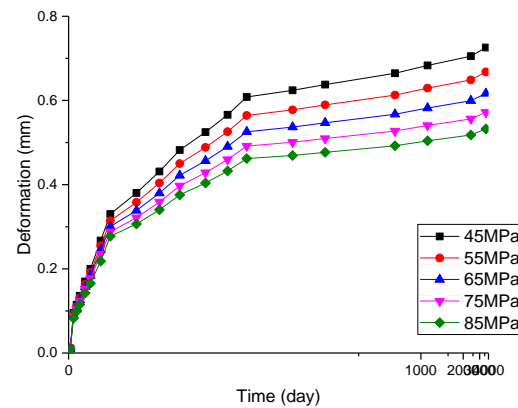
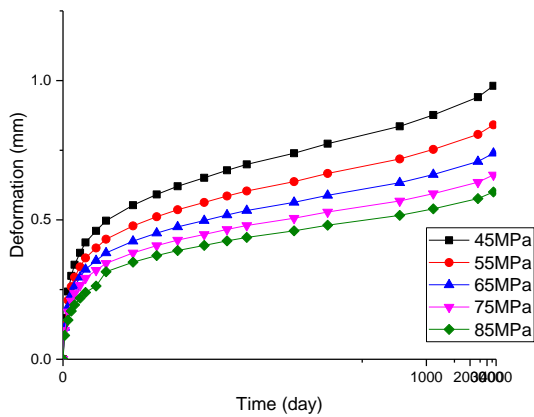
319

320 **Figure 11.** Comparison between theoretical, numerical and experimental results of time-dependent
 321 behaviour for 180-day

322 **6.5 Parametric study**

323 **6.5.1 Concrete compressive strength**

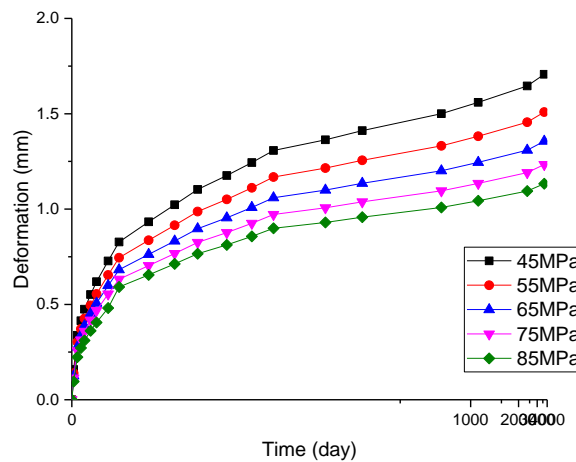
324 The material property is a key factor that influences time-dependent behaviour of prestressed concrete
 325 [6]. Therefore, various concrete compressive strengths of sleeper were studied to determine their
 326 performance. Based on the validated finite element model, concrete strengths of 45MPa, 55MPa,
 327 65MPa, 75MPa, 85MPa are researched through a parametric study. The various concrete strength
 328 results are plotted in **Figure 12**. This figure compares deformation due to time-dependent behaviour
 329 with concrete compressive strength between 45MPa to 85MPa. It can be seen that the time-dependent
 330 behaviour, both of creep and shrinkage, is inversely proportional with the development of concrete
 331 strength. The results comply with theoretical predictions. From **Figure 12**, it can be seen that the
 332 maximum difference of time-dependent deformation between concrete strength 45MPa and 85MPa is
 333 0.574mm (42.3%). The deformation is reduced by almost 10% with concrete strength increasing to
 334 10Mpa.



335

336 (a) creep deformation in various strength

(b) shrinkage deformation in various strength



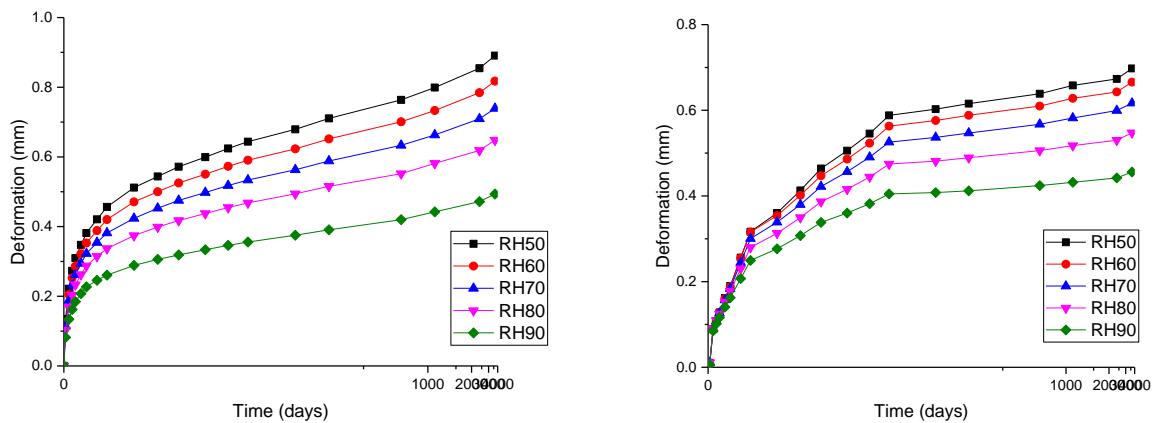
337

338 (c) total time-dependent deformation in various concrete strength

339 **Figure 12.** Parametric study of time-dependent behaviour in various concrete strength

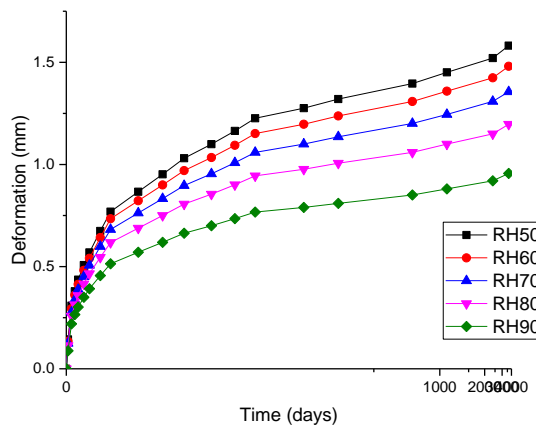
340 **6.5.2 Relative humidity**

341 According to preview research, the most significant parameters affect creep and shrinkage are the
 342 concrete strength and relative humidity [6]. Therefore, the analysis of relative humidity is conducted.
 343 Based on the validated finite element model, the relative humidity of 50%, 60%, 70%, 80%, and 90%
 344 are studied. **Figure 13** illustrates the relationships between different relative humidity and time-
 345 dependent behaviour. This figure compares deformation due to time-dependent behaviour with relative
 346 humidity between 50% to 90%. It can be seen that the deformation tends to be higher when the relative
 347 humidity reduces. The difference of total deformation between 50% and 90% is up to 46.13%. In
 348 comparison creep and shrinkage deformation, creep has more influence by relative humidity. The
 349 difference of creep deformation between 50% and 90% is 53.74%, whereas the difference of shrinkage
 350 deformation is 39.19%. It is noted that the relative humidity is more likely to affect the performance
 351 of railway sleepers than concrete strength.



352
 353 (a) creep deformation in various humidity

(b) shrinkage deformation in various humidity



354
 355 (c) total time-dependent deformation in various relative humidity

356 **Figure 13.** Parametric study of time-dependent behaviour in various relative humidity

357 6.5.3 Loss of prestress

358 Analysis of the long-term loss of prestress is an important part of the railway sleeper design process.
 359 In many prestressed concrete structures design process, the loss of prestress is a controlling parameter.
 360 The prestress loss could result in undesired deflections and cracking under service conditions. Loss of
 361 prestress occurs in two stages: loss at transfer and long-term loss. The immediate loss could be caused
 362 by anchorage, friction, and seating. The long-term loss is most due to interrelated effects of creep and
 363 shrinkage on concrete, and relaxation of steel tendons.

364 The Eurocode 2 [29] describes predict methods of loss due to time-dependent behaviour.

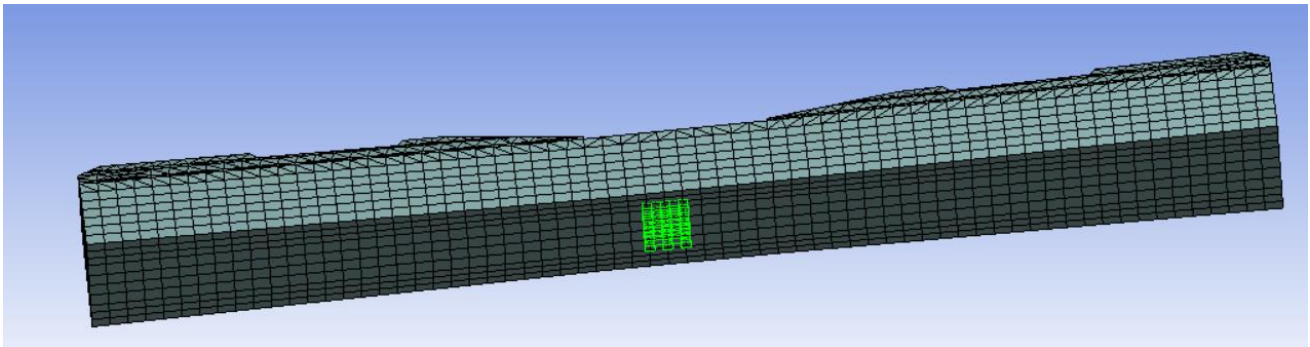
365 Loss due to creep: $Loss = \sigma_c \frac{E_s}{E_{cm}} \varphi$

366 Loss due to shrinkage: $Loss = \varepsilon_{cs} E_s A_{ps}$

367 Loss due to relaxation: $Loss = \Delta\sigma_{pr} A_{ps}$

368 The bottom part of midspan of the sleeper is selected as typical position to investigate the loss of
 369 prestress for numerical simulation (shown in **Figure 13**). The *Normal Stress* is used to checked the
 370 remained prestress in numerical model in different periods. The ratios of remained prestress and initial
 371 prestress are calculated in order to generate loss percentage. **Figure 14** illustrates the theoretical and
 372 numerical results of results of loss of prestress.

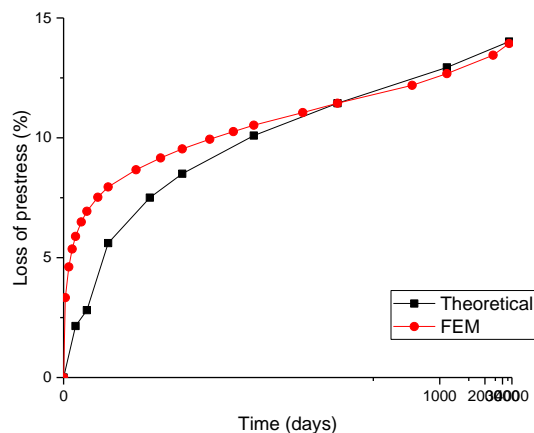
373



374

375 **Figure 13.** Typical position on numerical sleeper model for loss of prestress investigation

376



377

378 **Figure 14.** Comparison between theoretical and numerical results of loss of prestress

379 The numerical results comply with theoretical prediction. The loss of prestress exists along the whole
 380 life of railway sleepers. According to the experience of amount of preview research, the final value of
 381 remained prestress is only about 75% of the initial prestress [31]. In this study, the predicted loss of
 382 prestress is around 14%. The results can be used in further research to investigate the capacity of the
 383 railway sleeper.

384 7 Conclusion

385 Railway sleeper is one of the most important part in conventional track structure. Performance of
 386 prestressed concrete sleeper is influenced by time-dependent behaviour like other concrete structure.
 387 The deformation caused by creep and shrinkage can significantly influence the critical dimension of
 388 railway sleepers. Time-dependent behaviour of prestressed concrete sleepers is commonly related to
 389 material properties, environmental conditions, axle loads, and dynamic loads etc. A series of problems
 390 could be caused by time-dependent behaviour including dimension change, loss of prestress, cracks,
 391 deterioration, and decrease of capacity. The main effect of creep and shrinkage on railway sleeper
 392 happens in early-age service. First two months, the deformation due to time-dependent behaviour could
 393 reach 60% of total deformation. After 3 years, the deformation achieves 95% of total deformation and
 394 increasement becomes very slow and stable.

395 This paper presents the finite element results of Chinese Type III prestressed concrete sleeper analysis
 396 on the time-dependent behaviour. An experimental program was set up and completed where the
 397 critical dimension of five Chinese type III prestressed concrete sleepers were measured for 180 days
 398 in order to calibrate creep and shrinkage numerical models. This paper also introduces theoretical creep
 399 and shrinkage prediction methods based on Eurocode 2. The finite element model has been established
 400 and validated using comprehensive experimental data. The simulation shows great agreement in
 401 comparison with the theoretical and experimental results. The numerical results show that the creep
 402 and shrinkage deformation predicted by the numerical model are very close to 180-day experimental
 403 results. For 10-year prediction, numerical results are also very close to theoretical results which
 404 maximum error less than 13.46%. The relative humidity is also an important factor that influences
 405 creep and shrinkage. However, it is also very hard to control. In experiment, the relative humidity was
 406 not permanent during long-term measurement. It could be the reason that induces errors between
 407 experimental, theoretical, and numerical results.

408 In summary, for time-dependent behaviour, the relative humidity and concrete strength are the most
409 influential factors. They largely influence creep and shrinkage. The parametric study highlights the
410 effect of concrete strength, relative humidity, and loss of prestress. The parametric study indicates the
411 increment of the concrete strength reduces time-dependent deformation and it provides a guide that
412 railway engineer determines strength of sleeper when considering time-dependent behaviour. In
413 addition, reduction of water-cement ratio will decrease time-dependent deformation. The
414 environmental factors such as relative humidity needs to be considered comprehensively, because the
415 relative humidity is more likely to affect the performance of railway sleepers than concrete strength.
416 Dry climates usually result in more deformation due to creep and shrinkage. This opinion gives an
417 instruction for railway sleepers serviced in harsh environments (dry climates area). In this situation, it
418 is suggested that periodically sprays water on sleepers as maintenance in order to keep railway track
419 moisture. The parametric study also reveals percentage of the prestress loss in different periods, which
420 helps inspection of prestressed concrete sleepers in railway system.

421 In practice, the problems on prestressed concrete sleepers associated with time-dependent behaviour
422 can be: (a) change of railway sleeper geometry and influence rail gauge; (b) Reduction of sleeper's
423 loading capacity; (c) loss of prestress; (d) cracking on surface of railway sleepers. The major cause of
424 these problems is due to creep and shrinkage. These problems could result in serious consequence like
425 train derailment, increase of maintenance cost, service life of railway sleepers will reduce etc. It is
426 necessary to investigate time-dependent behaviour and find a reliable method to estimate the potential
427 effects on railway track system to avoid accidents. This paper presents the numerical analysis on time-
428 dependent behaviour. It finds the main parameters affect time-dependent behaviour, and they are also
429 applied in FE model to evaluate the performance of railway sleepers. The experimental results have a
430 good agreement with numerical results that indicate the FE model is reliable. For the further research
431 on creep and shrinkage, more parameters like load conditions, different materials, support conditions
432 [32-36] will be reviewed to evaluate the performance of railway sleepers under various conditions.

433 This article proposes the reliability concepts and rationale associated with the development of time-
434 dependent behaviour prediction methods. It reinforces the fundamental design guideline for prestressed
435 concrete sleepers to optimally suit any local track. This paper addresses the importance challenge
436 towards truly realistic condition-based predictive track maintenance. The outcome can be applied in
437 long-term railway infrastructure maintenance, concrete manufacturer factory, design code. The insights
438 will enhance the inspection of long-term serviced sleepers and improve track maintenance.

439

440 **Acknowledge**

441 The authors are grateful to Track engineering and Operations for Future Uncertainties (TOFU) Lab,
442 University of Birmingham for support throughout this study. The authors would like to thank the
443 Commission for H2020-MSCA-RISE, Project No. 691135 "RISEN: Rail Infrastructure Systems
444 Engineering Network" (www.risen2rail.eu). Also, the first author wishes to thank the Tsinghua
445 University, the China Academy of Railway Science (CARS) for the collaborative project. Valuable
446 comments and support from Dr Ping Liu and Dr Chayut Ngamkhanong are acknowledged.

447

448

449

450 **References**

- 451 1. S. Kaewunruen, A.M. Remennikov, Impact capacity of railway prestressed concrete sleepers,
452 Engineering Failure Analysis. 16 (2009) 1520–1532.
- 453 2. R. You, D. Li, C. Ngamkhanong, R. Janeliukstis, S. Kaewunruen, Fatigue Life Assessment
454 Method for Prestressed concrete sleepers, Frontiers in Built Environment. 3 (2017) 1–13.
- 455 3. C. Ngamkhanong, D. Li, S. Kaewunruen, Impact capacity reduction in railway prestressed
456 concrete sleepers with vertical holes, IOP Conference Series: Materials. (2017).
- 457 4. S. Kaewunruen, C. Ngamkhanong, P. Sengsri, M. Ishida, On Hogging Bending Test
458 Specifications of Railway Composite Sleepers and Bearers. Frontiers in Built Environment. 6
459 (2020).
- 460 5. P. Liu, S. Kaewunruen, D. Zhao, S. Wang, Investigation of the Dynamic Buckling of Spherical
461 Shell Structures Due to Subsea Collisions, Applied sciences. 8(7) (2018) 1148-52.
- 462 6. D. Li, S. Kaewunruen, P. Robery, A.M. Remennikov, Parametric studies into creep and shrinkage
463 characteristics in railway prestressed concrete sleepers. Frontiers in Built Environment. 6 (2020)
464 130.
- 465 7. P. Liu, S. Kaewunruen, B. Tang, Dynamic Pressure Analysis of Hemispherical Shell Vibrating
466 in Unbounded Compressible Fluid, Applied sciences. 8(10) (2018) 1938-42.
- 467 8. D. Li, S. Kaewunruen, Mechanical properties of concrete with recycled composite and plastic
468 aggregates. International Journal of GEOMATE. 17 (60) (2019) 231-38.
- 469 9. D. Li, S. Kaewunruen, P. Robery, A.M. Remennikov, Creep and Shrinkage Effects on Railway
470 Prestressed Concrete Sleepers. ICRT 2017: Railway Development, Operations, and
471 Maintenance. (2018) 394-405.
- 472 10. P. Liu, S. Kaewunruen, B. Tang, Dynamic Pressure Analysis of Hemispherical Shell Vibrating
473 in Unbounded Compressible Fluid, Applied sciences. 8(10) (2018) 1938-42.
- 474 11. X. Huang, J. Ge, S. Kaewunruen, Q. Su. The Self-Sealing Capacity of Environmentally Friendly,
475 Highly Damped, Fibre-Reinforced Concrete Materials. 13(2) (2020) 298.
- 476 12. G. Q. Jing, P. Aela, H. Fu, M. Esmaeili, Numerical and Experimental Analysis of Lateral
477 Resistance of Block Sleeper on Ballasted Tracks. International Journal of Geomechanics, 20(6)
478 (2020).
- 479 13. R. Janeliukstis, S. Ručevskis, S. Kaewunruen, Mode shape curvature squares method for crack
480 detection in railway prestressed concrete sleepers, Engineering Failure Analysis. 105 (2019) 386-
481 401.
- 482 14. J. Sadeghi, P. Barati. Comparisons of the mechanical properties of timber, steel and concrete
483 sleepers, Structure and Infrastructure Engineering 8 (2012).
- 484 15. C. Ngamkhanong, S. Kaewunruen, Influence of prestress losses on the dynamic over static
485 capacity ratios of railway concrete sleepers, in SynerCrete'18 International Conference on
486 Interdisciplinary Approaches, RILEM Publications S.A.R.L., Paris France. (2018) 925-30.
- 487 16. S. Kaewunruen, C. Ngamkhanong, J. Ng, Influence of time-dependent material degradation on
488 life cycle serviceability of interspersed railway tracks due to moving train loads, Engineering
489 Structures. 199 (2019).
- 490 17. R. You, K. Goto, C. Ngamkhanong, S. Kaewunruen, Nonlinear finite element analysis for
491 structural capacity of railway prestressed concrete sleepers with rail seat abrasion, Engineering
492 Failure Analysis. 95 (2019) 47-65.
- 493 18. C. Ngamkhanong, D. Li, A Remennikov, S. Kaewunruen, Capacity reduction in railway
494 prestressed concrete sleepers due to dynamic abrasions, 15th East-Asia Pacific Conference on
495 Structural Engineering and Construction. (2017).
- 496 19. C. Ngamkhanong, D. Li, A.M. Remennikov, S. Kaewunruen, Dynamic Capacity Reduction of
497 Railway Prestressed Concrete Sleepers due to Surface Abrasions Considering the Effects of

- 498 Strain Rate and Prestressing Losses. *International Journal of Structural Stability and Dynamics*,
499 19(1) (2019).
- 500 20. D. Li, S. Kaewunruen, Robery, P, Early-age responses of railway prestressed concrete sleepers
501 to creep and shrinkage, in *Proceedings of the 2nd International RILEM/COST Conference on*
502 *Early Age Cracking and Serviceability*. (2018) 567-72.
- 503 21. A. M. Remennikov, M. H. Murray, S. Kaewunruen, Reliability-based conversion of a structural
504 design code for railway prestressed concrete sleepers, *Journal of Rail and Rapid Transit*. 226(2)
505 (2011) 155-73.
- 506 22. W. Ferdous, A. Manalo, Failures of mainline railway sleepers and suggested remedies – Review
507 of current practice, *Engineering Failure Analysis*. 44 (2014) 17-35.
- 508 23. J. Sadeghi. Field investigation on dynamics of railway track pre-stressed concrete sleepers"
509 *Advances in Structural Engineering* 13.1 (2010).
- 510 24. J. Sadeghi, P. Barati. Experimental evaluation of accuracy of current practices in analysis and
511 design of railway track sleepers, *Canadian Journal of Civil Engineering* 35.9 (2008).
- 512 25. D. Li, S. Kaewunruen, Effect of Extreme Climate on Topology of Railway Prestressed Concrete
513 Sleepers, *Climate*. 7(1) (2019) 17.
- 514 26. W. He. Creep and Shrinkage of High-Performance Concrete and Prediction of Long-Term
515 Camber of Prestressed Bridge Girders, Iowa State University. 2013.
- 516 27. K. A. Byle, H. Burns, R. Carrasquillo. Time-dependent deformation behaviour of prestressed
517 high-performance concrete bridge beams. The University of Texas at Austin. 1997.
- 518 28. M. Lopez. Creep and shrinkage of high-performance lightweight concrete: A multi-scale
519 investigation. Georgia Institute of Technology, 2005.
- 520 29. EN1992-2. Design of concrete structures. Part 2: concrete bridges design and detailing rules.
521 Brussels; European Committee for standardization, 2005.
- 522 30. E. C. f. Standardization, Railway applications-track-concrete sleepers and bearers part 2:
523 Prestressed monoblock sleepers, 2009.
- 524 31. P. Bhatt. Prestressed concrete design to Eurocodes, first edn., Abington: Spon Press (UK), 2011.
- 525 32. J. A. Zakeri, J. Sadeghi. Field investigation on load distribution and deflections of railway track
526 sleepers[J]. *Journal of Mechanical Science and Technology*, 21(12) (2007): 1948.
- 527 33. J. Sadeghi, A. R. Tolou Kian, and A. Shater Khabbazi. Improvement of mechanical properties
528 of railway track concrete sleepers using steel fibres. *Journal of Materials in Civil Engineering*
529 28.11 (2016): 04016131.
- 530 34. S. Kaewunruen, and A. M. Remennikov. Investigation of free vibrations of voided concrete
531 sleepers in railway track system. *Proceedings of the Institution of Mechanical Engineers, Part F:*
532 *Journal of Rail and Rapid Transit* 221.4 (2007): 495-507.
- 533 35. Taherinezhad, J., Sofi, M., Mendis, P. A., and Ngo, T. A Review of Behaviour of Prestressed
534 Concrete Sleepers, *Electronic Journal of Structural Engineering*, 13(2): 1-16, (2013).
- 535 36. Kaewunruen, S., Ngamkhanong, C., Lim, C.H., Damage and failure modes of railway prestressed
536 concrete sleepers with holes/web openings subject to impact loading conditions, *Engineering*
537 *Structures*, 176, 840-848, (2018). doi:10.1016/j.engstruct.2018.09.057